Novel Hydrophobic Coatings for Soiling Mitigation in the PV Industry: Durability and Anti-Soiling Demonstrations

Benjamin Strauss [1], Fabiana Lisco[2], and Farwah Bukhari[2], John M. Walls [2] and Kurt L. Barth [1]

[1] Colorado State University, NSF I/UCRC for Next Generation Photovoltaics, Fort Collins, CO 80526 United States

[2] Crest, Loughborough University, Loughborough, United Kingdom, Le11 3tu

Abstract — **Soiling, the buildup of debris on the front-side of a solar module, can significantly reduce the power production due to a reduction in transmitted light to the underlying solar cell. A potential solution to soiling mitigation involves the use of hydrophobic coatings. In this study commercially available hydrophobic coatings found in non-PV sectors of industry are investigated. Through the use of anti-soiling and standardized durability testing procedures, the suitability of these existing hydrophobic coatings for use in the PV industry is quantitatively analyzed.**

Index Terms – **solar energy, photovoltaic cells, coatings, solar panels**

I. Introduction

Roughly 5% of electricity generated world-wide comes from solar and wind technology [1]. One of the quickest growing renewable energy technologies is photovoltaic (PV) solar power, having a global growth rate of 40% per year over the last 20 years [2]**;** this is due largely to cheaper solar-produced electricity. While the growth of PV is impressive and leads to a promising outlook for the future of energy production, it is not without its challenges.

Soiling, the build-up of dust and debris on the surface of a solar module, can significantly reduce the amount of sunlight that reaches the underlying solar cell. Decreases in solar module energy production of 20-30% have been observed in arid-desert climates [3], regions where sunlight is most intense and abundant. Therefore, soiling is a major power output reduction mechanism and has become a topic of significant concern [4]–[7]. Current soiling mitigation techniques involve some type of mechanical cleaning process, either manual or automated, which can be highly water and cost intensive. A solution to soil mitigation is of interest among the PV research community, and one approach is through the use of anti-soiling, specifically hydrophobic, coatings.

Various non-PV industrial sectors including automotive, ophthalmic, and electronics, utilize hydrophobic coatings to enhance the performance of their products. One or more of these commercially available hydrophobic coatings may be adaptable to the PV industry for soiling mitigation purposes. In a previous study, we investigated and characterized ten commercially available hydrophobic coatings (labeled as Coating A – J for company anonymity) using a preliminary water contact angle (WCA) and roll-off angle (RoA) screening procedure [8]. With defined WCA and RoA performance cut-off criteria of 110° and 25° respectively. From those studies, a group of five candidate coatings were selected for further anti-soiling research. These coatings are labeled as Coating E, I(s), I(d), J and F. Coating I was applied using both a spray and dip-coating method, hence the respective I(s) and I(d) nomenclature. Coating J was the only one marketed for PV-specific application amongst all the obtained commercially available hydrophobic coatings.

Therefore, the current study quantitatively examines the durability and anti-soiling properties of these five commercially available hydrophobic coatings to better understand the suitability for soiling reduction on PV modules.

II. Experimental Methods and Approach

A. Durability Testing Procedure

A standardized durability testing procedure was developed at Loughborough University specifically for hydrophobic coatings on solar cover glass [9]. This accelerated test simulates the harsh environmental conditions experienced by a solar module throughout its lifetime. For each of the five hydrophobic coating formulations, ten (5x5) cm and ten (1x1) cm glass substrates were fabricated. PPG Starphire glass substrates were cleaned in an ultrasonic bath process before the coatings were applied. All fabricated samples were then initially characterized using WCA and RoA measurements. The samples were then exposed to a variety of external stressors in order to induce degradation of the coating.

The primary durability testing procedures included in this paper are a damp heat test of 85 C and 85 % relative humidity (IEC 61215, MQT 13) run up to 1000 hours, and accelerated UV exposure (>2x IEC 61215, MQT 10). UV testing is done in a QUV chamber with UVA-30 lamps and is completed through 2000 hours, which roughly translates to about two and a half years of outdoor sun exposure. An extended timeframe of accelerated exposure is ideal; however, 2000 hours is a preliminary testing duration. Elevated temperatures (~60°C) do occur during UV exposure due to residual heat from the bulb, but at a much lower value than that of DH (85°C). Samples of each coating formulation were pulled from each test at various durations (e.g. 250 hrs, 500 hrs, 1000 hrs) to observe any induced degradation. Quantification techniques included in this paper are WCA and RoA performance.

B. Anti-Soiling Testing Procedure

In order to quantify the anti-soiling properties of candidate hydrophobic coatings, a dust deposition and dust removal experimental procedure was developed utilizing an artificial dust deposition chamber and a low-velocity forced air dust removal apparatus. The automated dust deposition chamber was fabricated to allow for uniform and repeatable deposition of dust onto a given (5x5) cm glass substrate (Figure 1). The basis of the chamber design was based on work by Mantha from Arizona State University [5]. A wind tunnel was fabricated to enable the generation of uniform low-velocity air profiles for dust removal. Arizona road test dust (ISO 12103-1 A2) was used as the dust medium. For this work, the dust was deposited under dry conditions with ambient relative humidity (RH) and room temperature during the deposition process within the soiling chamber. Under these conditions, the dust adhesion mechanisms are largely composed of Van der Waals (VDW) forces and any existing electrostatic attraction between the particles and the substrate surface [10]. Dust cementation, the more aggressive adhesion mechanism, is not induced during the dry-air deposition testing conditions as it requires the presence of liquid water.

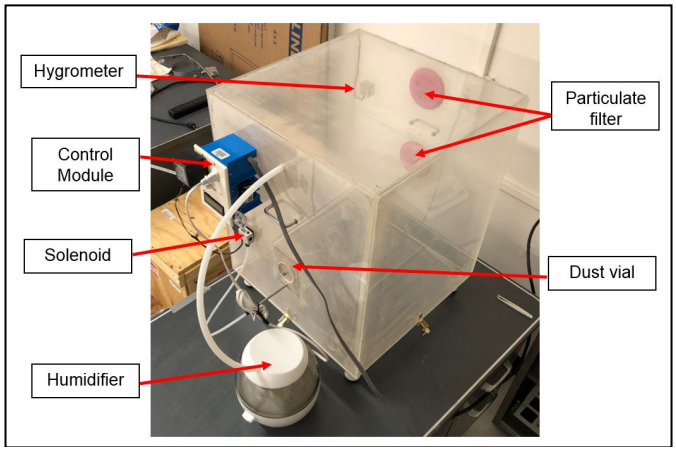

Fig.1. Artificial dust deposition chamber with labeled feature components.

Direct transmission measurements were used as the quantification technique for the anti-soiling testing procedure. Prior to each transmission reading, the tool was calibrated using a calibration control sample set aside from each batch of the fabricated samples. The spectrum of the light source spanned a 350-1050 nm wavelength range. Since the measurements were normalized against a clean calibration sample, the transmission data was reported as a single average value. Therefore, any losses in transmission represents losses due to soiling of the sample.

In preparation for the dry-air anti-soiling testing procedure, eight samples for Coatings E, F, I(d), I(s), and J were each fabricated on (5 x 5) cm Starphire glass substrates. Eight samples of uncoated glass were also fabricated to act as the control group. Baseline RoA and WCA measurements were then taken on the fabricated samples. The design of the artificial dust deposition chamber and the low-velocity wind tunnel apparatus allow for only one sample to be tested at a given time. Therefore, the testing was split up by coating formulation, with uncoated glass being the first to complete the dry-air anti-soiling testing procedure. The following step-by-step process describes one trial of this testing procedure. The sample is coated with the particular coating, cured and measured for transmission. After the initial transmission measurement, the sample is placed onto the substrate holder located within the dust chamber. 2.5 g of Arizona test dust is loaded into the dust vial. With a line pressure of 120 psi and a burst duration of 2 seconds, the dust cloud is then suspended above the sample. The dust is then allowed to settle onto the sample for a period of 10 minutes following the compressed nitrogen burst. The sample is then carefully removed from the chamber to not disrupt the dust and a direct transmission measurement is taken using the methods previously described. The sample is then carefully placed into the wind tunnel apparatus, where it is exposed to 30 seconds of a low-velocity air stream at 5.3 m/s. This wind speed was calculated as the average annual wind speed at 5 major utility scale PV plants across the world [11]. The sample is then measured again for transmission. This completes one trial of the dry-air anti-soiling testing procedure. All samples for each coating variation and the uncoated glass were run through this process resulting in 40 trials.

Statistical analysis was then run on the transmission data to identify any significant differences in dust removal (i.e. soiling reduction) existent between the coated vs uncoated samples. Both parametric and non-parametric two-sample t-tests were used in the statistical analysis depending on the distribution behavior of the 8 samples for each coating. A significance level of 5% was used across the board for all comparisons.

III. Results and Discussion

A. Damp Heat Results

The WCA and RoA results for DH exposure are reported through a duration of 1000 hours and can be seen in Figure 2. Note that the x-axes are non-linear and follow the durations at which the samples were pulled for characterization. Referencing Figure 2a, all coatings apart from Coating J demonstrated stable WCA (target criteria represented by the red dashed line at 110º) up though 300 hours of DH exposure. The WCA for Coating J fell rapidly after 50 hours of DH and continued dropping until it leveled out around a WCA of 40º after 300 hours exposure. Coating F experienced a rapid decline in WCA after 300 hours of exposure. The WCA for coatings I(s), I(d), and E remained stable throughout the 1000 hours of DH. Figure 2b shows the RoA

data up through 1000 hours of DH exposure; the red dashed line marks the desired criteria of 25°. A general increasing trend was observed in RoA for all five hydrophobic coatings throughout the testing duration. With the exception of coating E, the remaining coatings measured an "as received" RoA at or below 25°. Almost immediately, the RoA for coatings E, F, and J increased above the desired criteria. Coating I, both spray (s) and dip (d) applied, demonstrated the longest duration of stable RoA through 400 hours of DH exposure, at which point it began rapidly increasing.

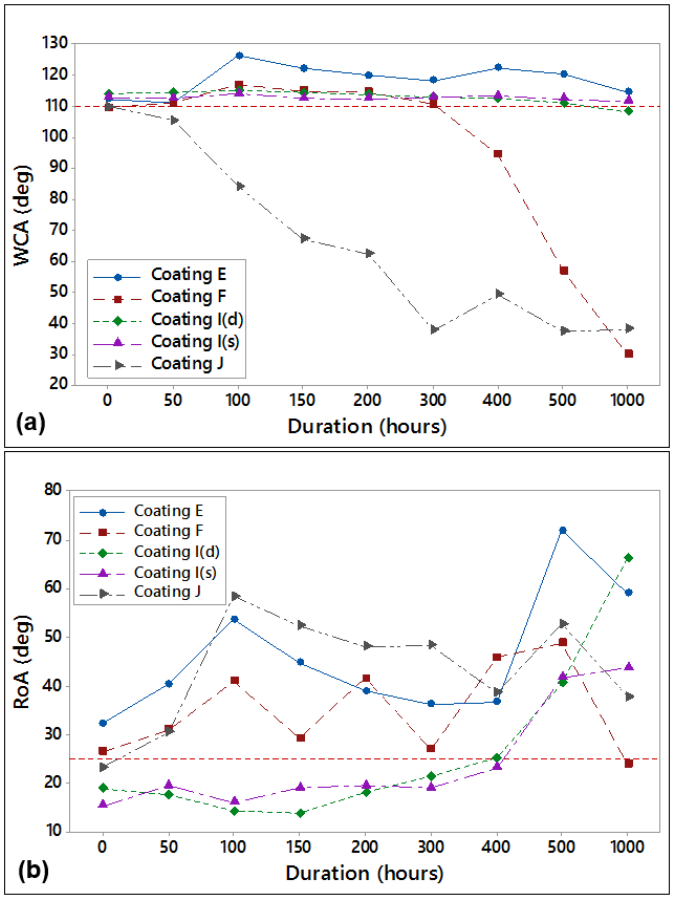

Fig. 2. a) WCA and (b) RoA data as a function of exposure duration to DH for the five candidate coatings.

B. Accelerated UV Results

The WCA and RoA was measured up through 2000 hours of UV exposure and is reported in Figure 3. The red dashed lines once again represent the desired WCA and RoA criteria of 110° and 25° respectively. The x-axes are also non-linear and follow the durations at which the samples were pulled for characterization. Referencing Figure 3a, all coatings demonstrated a fairly stable WCA up through 500 hours UV exposure. Coating J, as seen in the DH exposure testing, was the first to see significant decline in WCA. Coatings I(s), I(d), and F were stable up to 1000 hours of UV, at which point they began dropping off. Coating E saw an increase in WCA after the initialization of the testing and remained relatively stable in WCA throughout the 2000 hours of UV exposure. Similar to the trend observed in DH, a general increase in RoA was observed across all five coatings (Figure 3b). All coatings, with the exception of Coating E, started near or below the criteria of 25°. Coatings I(s) and I(d) showed relative stability in RoA up through 450 hours of UV exposure. Coating E saw the most dramatic increase in RoA after only 50 hours, however remained relatively stable thereafter up to 1000 hours. Coatings F and J surpassed the 25° criteria after roughly 100 hours of UV exposure.

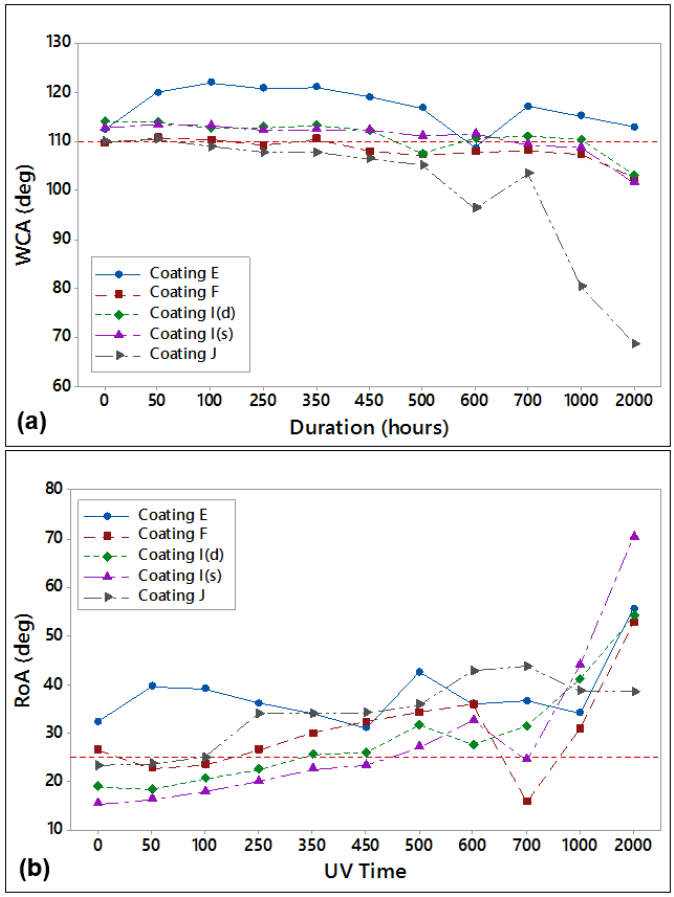

Fig. 3. (a) WCA and (b) RoA data as a function of exposure duration to UV for the five candidate coatings.

From the accelerated UV and DH durability testing, Coating I(s) and I(d) demonstrated both stability in WCA and prolonged stability in RoA when compared the alternative candidate coatings. Further investigation is needed using SEM imaging and XPS surface analysis to better understand the degradation mechanisms occurring in the hydrophobic coatings as a function of UV and DH exposure.

C. Dry-Air Anti-Soiling Performance

During the RoA characterization stage of the dry-air testing procedure, a significant increase in RoA for Coating E was observed, reaching angles around 45-50°. Having observed a much lower RoA in the past, a new batch of Coating E was applied using the same manufactured-suggested application procedure, glass substrate, and cure time as before. The RoA measured from 35-50° for this batch. This process was repeated a few times with similar results. Coating E was therefore eliminated from further anti-soiling testing. Inconsistent and often high RoA measurements also provided objective justification in the elimination of Coating E.

To quantify the soiling losses, transmission measurements were taken after dust deposition and again after the forced air removal. All transmission measurements were normalized by a respective clean calibration sample for each coating and the uncoated substrates. As seen in Figure 4, all 4 coating variations had a median post-dust deposition transparency value that fell within 3% of the plain glass (PG) median value of 72.8%, marked by the red dashed line. Coatings J, I(s), and I(d) showed no statistically significant difference in post-dust transmission when compared to PG. With a P-value of 0.014, Coating F did demonstrate a larger loss in transparency after the dust deposition. Executing the dry-air/low-velocity testing procedure took about 4 hours for each coating variation, so approximately 15-20 days were needed to complete the testing. Therefore, the difference detected in Coating F when compared to PG may be attributed to day-to-day variation in ambient conditions and deposition variability in the artificial dust chamber.

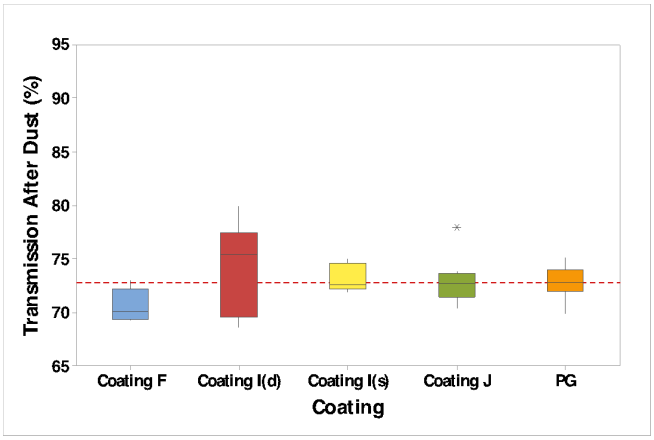

Fig. 4. Standard box-plot of transmission measurements taken after dust deposition for each coating formulation and uncoated glass. All normalized using a clean calibration sample for each respective coating. Red dashed line represents median transmission value for plain uncoated glass.

Transmission measurements taken after the low-velocity air removal revealed statistically significant differences between all coatings and the uncoated glass substrates, with the highest P-value of 0.032 for Coating J. Figure 5 shows the box-plot distributions of soiled coating transmissions after exposure to low-velocity air removal (5.3 m/s). Coating F, although demonstrating a larger loss in transmission after dust deposition, showed the largest recovery in percent transmission after the air removal at 92.6%. Coatings I(s), I(d), and J had median post-air transmissions values of 86.5%, 83.6%, and 81.9% respectively, compared to uncoated glass with a median transmission of 80.2% marked by the red dashed line. Hydrophobic coatings reduce VDW forces due to their lower surface energy [11]. These forces are a dominant dust adhesion mechanism under dry dust deposition conditions. Therefore, reducing these interfacial forces leads to the greater transmission recovery observed with the hydrophobic coatings under constant low-velocity air removal. From these results, it can be stated with statistical significance that the hydrophobic coatings tested demonstrate anti-soiling properties when compared to uncoated solar cover-glass.

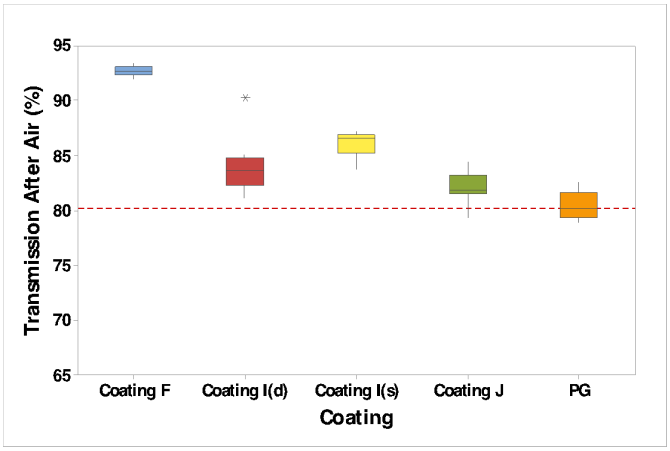

Fig. 5. Standard box-plot of transmission measurements taken after forced air removal for each coating formulation and uncoated glass. All normalized using a clean calibration sample for each respective coating. Red dashed line represents median transmission value for plain uncoated glass.

V. Summary

Significant progress has been made in developing and testing a viable anti-soiling coating. From this study, a commercially available hydrophobic coating formulation, Coating I(s,d), has demonstrated the ability to maintain sufficient water contact angle after UV and DH exposure testing. Coating I(s,d) also demonstrates a prolonged sufficient RoA when compared to the alternative hydrophobic coatings. All obtained hydrophobic coatings showed statistically significant anti-soiling properties when compared to plain uncoated glass under dry-air dust deposition. This supports the hypothesis that VDW dust adhesion forces are reduced on a hydrophobically coated surface due to the lowered surface energy. The series of tests

shared within this paper show promise for the near-term development of a robust anti-soiling coating with sufficient durability for economic commercial deployment.

Subsequent research efforts will include investigating coating degradation mechanisms seen under durability testing using SEM imaging and XPS analysis. The results from these tests are vital in understanding any morphological and chemical changes occurring within the coatings and will inform additional research efforts in optimizing the hydrophobic coating formulations/application for use in the PV industry. One of the strongest and more representative dust adhesion mechanisms seen in real-world PV is cementation [12]. Therefore, an anti-soiling testing procedure using high-humidity dust deposition conditions to achieve cementation will be developed and executed for the candidate hydrophobic coatings. Outdoor testing of the top performing coating, Coating I, will also be investigated at our solar test array at CSU to gain a qualitative understanding of real-world anti-soiling benefits.

REFERENCES

[1] BNEF, "New Energy Outlook 2017." p. 6, 2017.

[2] R. Fu *et al*., "U . S . Solar Photovoltaic System Cost Benchmark : Q1 2016 U . S . Solar Photovoltaic System Cost Benchmark : Q1 2016," *Nrel*, no. September, 2016.

[3] H. A. AlBusairi and H. J. Moller, "Performance evaluation of CdTe PV modules under natural outdoor conditions in Kuwait," *25th Eur. Photovolt. Sol. Energy Conf. Exhib. / 5th World Conf. Photovolt. Energy Convers. , 6-10 Sept. 2010 , Val. , Spain*, no. September, pp. 6–10, 2010.

[4] L. L. Kazmerski, M. Al Jardan, Y. Al Jnoobi, Y. Al Shaya, and J. J. John, "Ashes to ashes, dust to dust: Averting a potential showstopper for solar photovoltaics," *2014 IEEE 40th Photovolt. Spec. Conf. PVSC 2014*, pp. 187–192, 2014.

[5] Shanmukha Mantha, G. Tamizhmani, C.-C. Patrick Phelan, and C.-C. Liping Wang, "Development of Uniform Artificial Soil Deposition Techniques on Glass and Photovoltaic Coupons," 2016.

[6] L. R. de O. C. Lawrence L. Kazmerski, Antonia Sonio A.C., Christiana Brasil Maia, Marcelo Machado Viana, Suellen C. Costa, Pedro P. Brito, Claudio Dias Campos, Lauro V. Machado Neto, Sergio de Morais Hanriot, "Fundamental Studies of the Adhesion of Dust to PV Module," *IEEE J. Photovoltaics*, 2015.

[7] S. Bhaduri, S. Warade, J. J. John, B. Kavaipatti, and A. Kottantharayil, "Artificial dust deposition using water as carrier solvent for investigation of soiling losses in photovoltaic modules," in *Conference Record of the IEEE Photovoltaic Specialists Conference*, 2016.

[8] B. Strauss and K. Barth, "Investigating Solutions to Soiling Losses in the Photovoltaic Industry: A Characterization of Existing Commercial Hydrophobic Coatings," *Sol. Energy*, pp. 1–7, 2019.

[9] K. Isbilir, B. Maniscalco, R. Gottschalg, and J. M. Walls, "Test Methods for Hydrophobic Coatings on Solar Cover Glass," in *EU PVSEC 2017*, 2017.

[10] Y. Y. Quan and L. Z. Zhang, "Experimental investigation of the anti-dust effect of transparent hydrophobic coatings applied for solar cell covering glass," *Sol. Energy Mater. Sol. Cells*, vol. 160, no. August 2016, pp. 382–389, 2017.

[11] B. Strauss, "Investigating the Suitability of Existing Commercial Hydrophobic Coatings for Soiling Mitigation in the Photovoltaic Industry," ProQuest ETD, Publication Number 13813733, March, 2019.

[12] E. F. Cuddihy, "Theoretical considerations of soil retention," *Sol. Energy Mater.*, vol. 3, no. 1–2, pp. 21–33, 1980.